G.L. PANKANIN, J. BERLINSKI, R. CHMIELEWSKI

Warsaw University of Technology
Institute of Electronic Systems
Poland, e-mail: g.pankanin@ise.pw.edu.pl

SIMULATION OF KARMAN VORTEX STREET DEVELOPMENT USING A NEW MODEL

The article is devoted to the simulation of the Karman vortex street using an analytical model. The model has been described in detail in [1]. Fundamental quantities like velocity driving the vortex, vortex rotation and vortex rotation energy have been simulated. Also the influence of the fluid viscosity on the phenomena has been considered (analyzed). The results of the simulation have been compared with those obtained by application of other research methods. Considerable consistency has been reached.

Keywords: numerical modelling, simulation, Karman vortex street, vortex meter

1. INTRODUCTION

The phenomenological model of the Karman vortex street has been proposed in [1]. The model is based on fundamental mechanical equations describing hypothetical vortex development. The existence of the wedge-shaped stagnation region just downstream the bluff body has been taken as the fundamental assumption for the model. This assumption is based on Birkhoff's observations [2] and also on results of our own investigations carried out by the authors [3, 4]. Further considerations are based on simple analysis of velocity distribution in the duct confined by the walls. The problem of model verification by the experimentally obtained results is of great significance.

2. SHORT DESCRIPTION OF THE MODEL

As shown in Fig.1, the circular cylinder being the bluff body is appointed in the duct limited by the walls. Eddies originated on the bluff body surface grow up rolling downstream on the surface of the stagnation region. Succeeding layers are added to the vortex, hence its diameter and energy increase.

Due to varying vortex development conditions, the area downstream the bluff body has been divided into three zones:

- intensive development zone,
- stabilization zone,
- vortices decay zone.

A mathematical description of the vortex development in each of the mentioned zones has been performed. Also the influence of the fluid viscosity on the vortex development process has been described. Detailed equations describing the phenomena have been presented in [1].

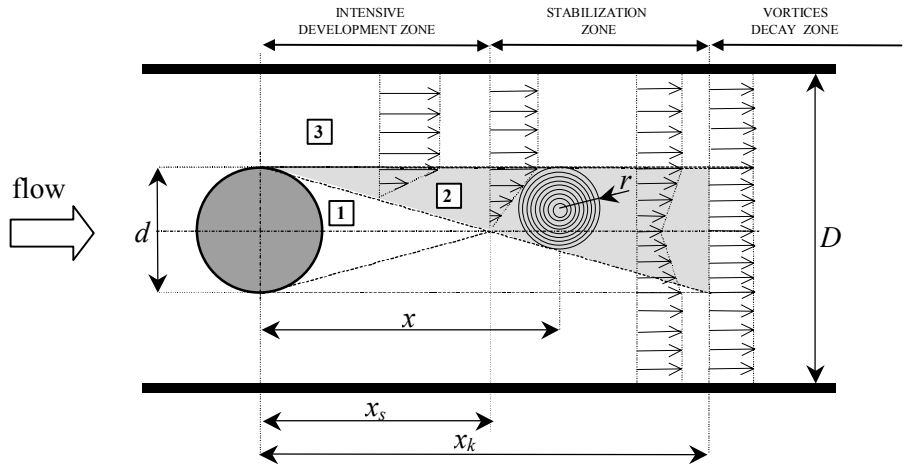

Fig. 1. Development of consecutive vortices downstream bluff body (1 - stagnation region, 2 - region of vortices development, 3 - region of steady velocity profile).

3. RESULTS OF SIMULATION

The phenomena occurring in the rectangular cross-section duct have been simulated, so the two-dimensional model presented in Fig.1 has been considered. The circular cylinder as the bluff body was located in the duct perpendicularly to the flow direction. The simulations have been carried out for steady flow velocity equal to1 m/s and for various values of blockage ratio d/D. It was assumed that the vortex radius increases linearly versus its current position. Vortex development in each zone has been split into 10 steps. One layer has been added to the vortex in each step. Numerical simulations for the model with non-viscous fluid and then for the model with viscous interaction among the fluid layers have been carried out.

3.1. Results of simulation for a model without viscous interaction

Variation of the flow velocity driving the vortex with the distance from the bluff body is shown in Fig. 2. As it is seen, the velocity strongly depends on the blockage ratio - especially in close neighbourhood of the bluff body. The considerable increase of this velocity (especially in the intensive development zone) for the greatest values of the blockage ratio results from strong damming effect. It can be underlined that the influence of the pipe walls is manifested by an increase of the driving velocity. The increase of the velocity **vpc** caused by the damming effect is favourable from the point of view of vortices energy. It is worth to note that a too high blockage ratio is disadvantageous because of boundary layer effects.

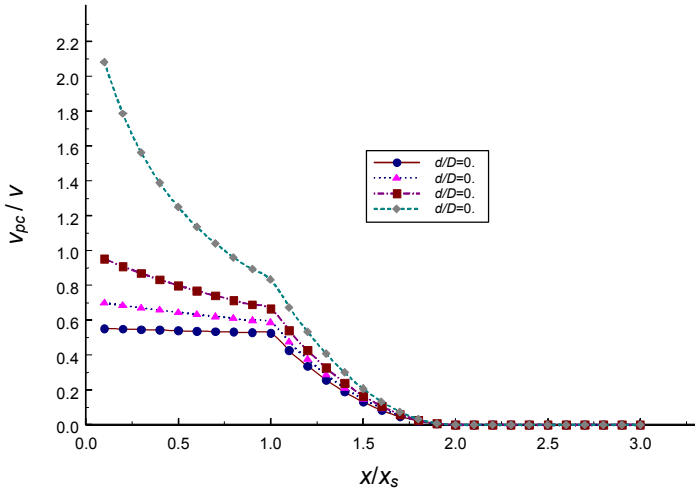

Fig. 2. Reduced flow velocity forcing the vortex vs. relative distance from the bluff body axis.

It is easy to remark that the velocity forcing the vortex decreases along the distance from the bluff body. It means that the vortex gets (energy) weaker and weaker. The forcing diminishes to zero when the vortex reaches the end of the stabilization zone ($x/x_s = 2$) - regardless of the blockage ratio.

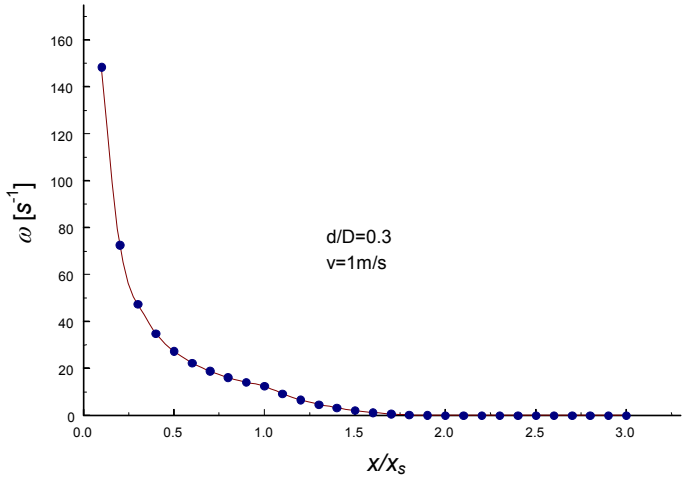

Fig. 3. Vortex angular velocity of the outer layer vs. current vortex location.

As seen in Fig. 3, the greatest angular velocity is achieved by the outer layers in the closest vicinity of the bluff body. The angular velocity of a currently added vortex layer results from the local flow velocity and the vortex radius. Due to the small vortex radius in the area close to the vortex origin, initial layers achieve considerably high values of angular velocity. As seen in the graph, consecutive layers reach gradually smaller angular velocities. At the end of the stabilization zone ($x/x_s = 2$), forcing of the layers decays and the added layers attain zero angular velocity.

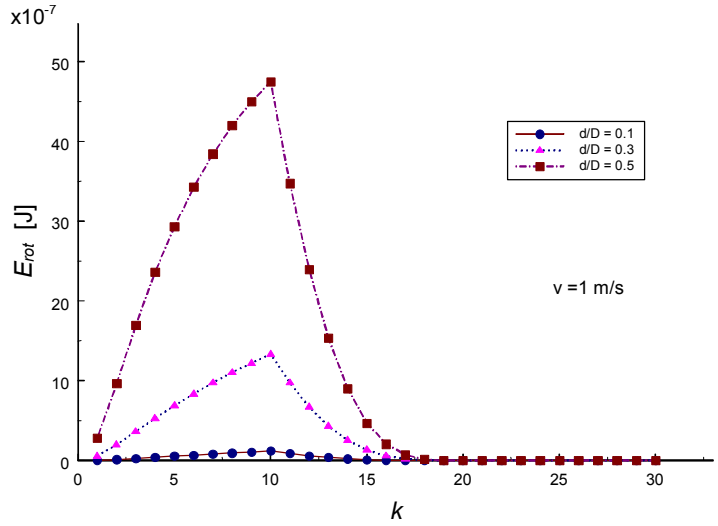

Fig.4. Distribution of rotation energy in the vortex.

Simulation results of rotation energy distribution in the vortex which are presented in Fig. 4. confirm the rapid vortex development in the whole intensive development zone ($k \leq 10$). Consecutively added layers have gradually higher energy. In the stabilization zone the rotation energy of every next layer gains lower rotation up to zero value at the end of the zone.

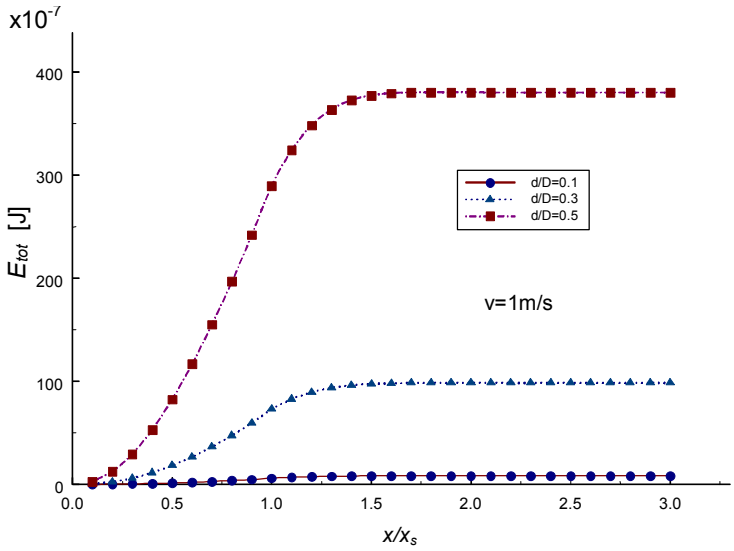

Fig. 5. Total rotation energy of the vortex as a function of current vortex position.

Total rotation energy being the sum of rotation energies of all layers is presented in Fig. 5. As it is seen, the vortex development appears at a limited distance from the vortex origin. The total rotation energy rapidly increases in the intensive development zone ($x/x_s \leq 1$) and partially in the stabilization zone ($1 \leq x/x_s \leq 2$). The vortex energy reaches the maximum value in the stabilization zone only. Considerable differences of the rotation energy for various blockage ratios are observed. The blockage ratio strongly influences the magnitude of the total rotation energy and the increase of the blockage ratio results in considerably higher value of the total energy.

3.2. Results of simulation for a model with viscous interaction

As mentioned in [5], the viscosity forces in real fluids are not only the reason of the vortex origin but also play a very important role in the vortex development. Viscous interaction between adjacent layers of different rotations tends to uniform rotations and also causes energy losses.

The effect of the adjoining layer's tendency to gradual equalization of their angular velocities is particularly visible in the case of the earliest generated layers - being close to the centre of the vortex. It is easy to explain this through the slight mass of the layers and - on the other hand - considerable differences in angular velocities of adjoining layers (Fig. 6).

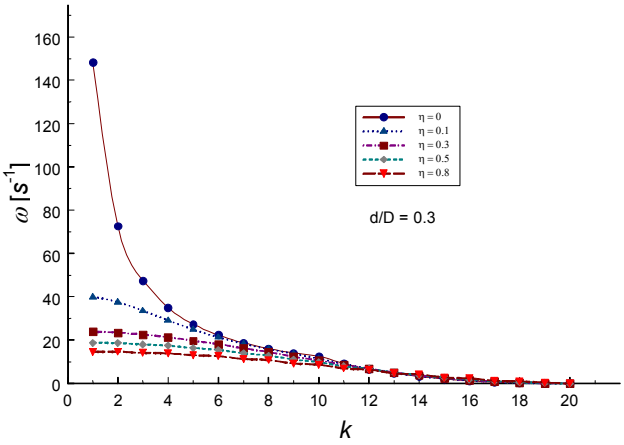

Fig.6. Distribution of layers rotation in vortex for various fluid viscosities (for the vortex turned up at the end of the stabilization zone).

The distribution of layer's rotation velocity in the vortex being in various distances from its origin presented in Fig.7 show that viscosity forces result in a considerable decrease of the rotation velocities along with the vortex development. It is also worth to remark that outer layers (generated in the stabilization zone) even slightly increase their rotation velocity - due to the viscosity forces.

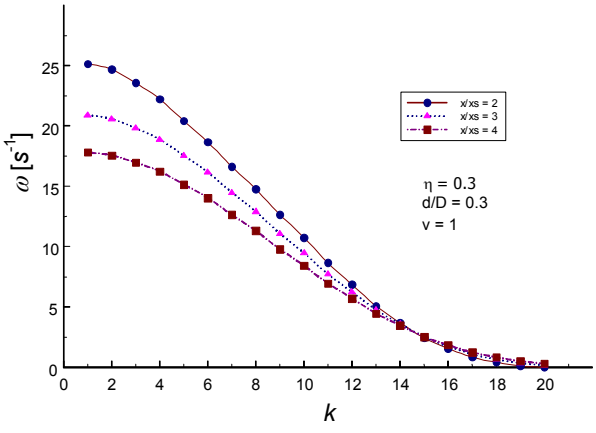

Fig.7. Distributions of layers rotation for the vortex being in various distances from its origin.

The influence of the liquid viscosity on the rotation energy distribution in the vortex is presented in Fig. 8. As it is easy to notice, the energy is concentrated mainly in the layers generated at the end of the intensive development zone and at` the beginning of the stabilization zone. The rotation energy decreases more intensively in the case when the liquid viscosity increases. It is worth to remark that energy distribution only slightly depends on the

liquid viscosity. Obviously a greater value of the viscosity results in higher energy losses and in stronger (more efficient) energy transmission towards the outer layers of the vortex.

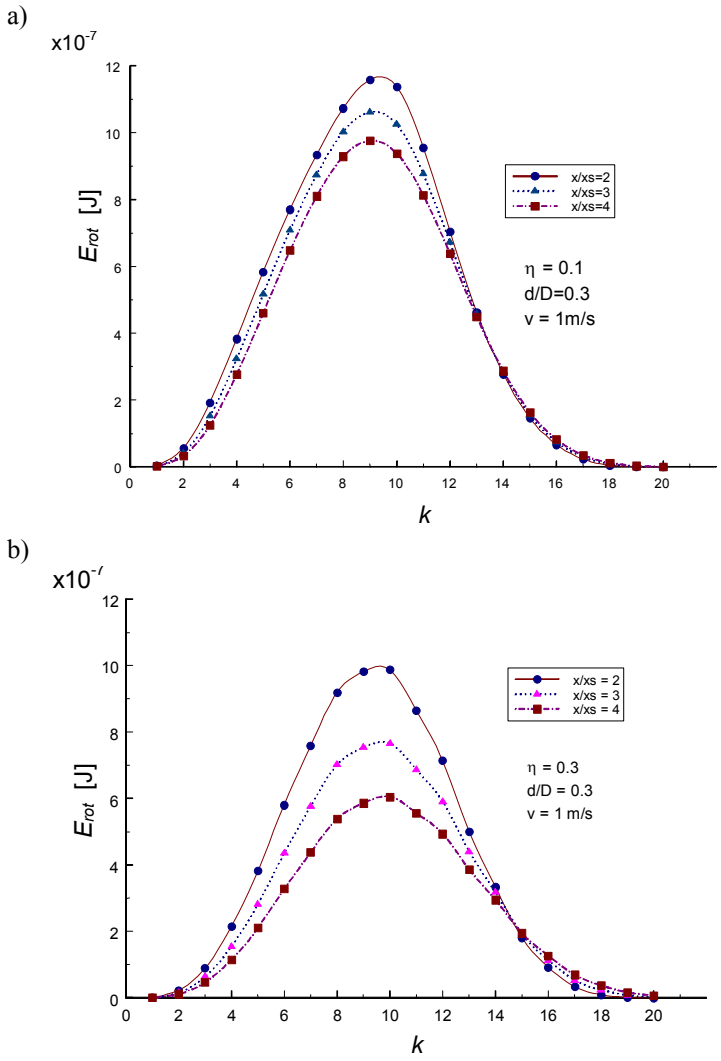

Fig. 8. Influence of liquid viscosity on the rotation energy distribution inside the vortex (for various distances from its origin).

The graph of the total rotation energy as a function of current vortex location for various liquid viscosities (Fig.9) confirms the existence of successive phases of the vortex development. In the first phase ($x/x_s < 1.4$) a rapid energy increase is observed. It is necessary to underline that the increase occurs not only in the vortex intensive development zone but also at the beginning of the stabilization zone. After the energy maximum is achieved, it decreases along with the vortex displacement. The rotation energy decrease strongly depends on the fluid viscosity. It is characteristic that in the region of vortex development, the growth of rotation energy almost does not depend on the fluid viscosity.

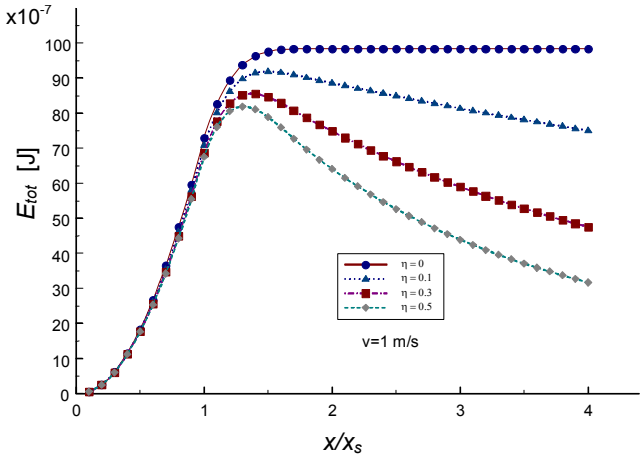

Fig. 9. Total rotation energy of the vortex as a function of the current vortex location.

4. COMPARISON OF SIMULATION WITH EXPERIMENTAL RESULTS

Results of simulation using the proposed model can be compared with the results of experimental investigations. The most important result of the simulation is the determination of the variation of the total rotation energy vs. the vortex distance from the origin. The graph presented in Fig. 9 shows that the vortex energy gradually increases along with the vortex displacement downstream the bluff body. At a certain distance from the bluff body it achieves its maximum and then slowly (depending on the fluid viscosity) decreases. The experimental data are presented in Fig. 10.

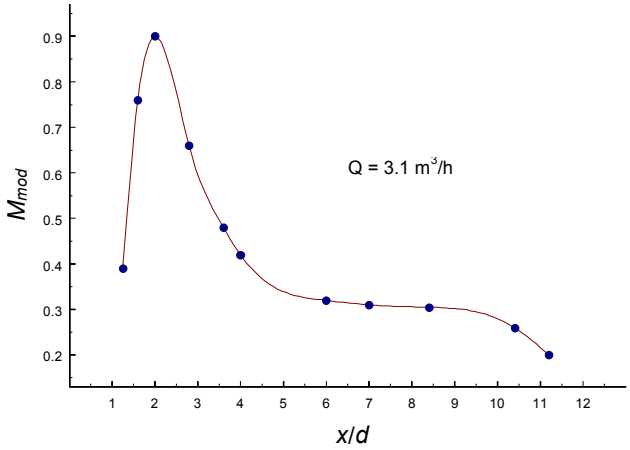

Fig.10. Influence of sensor location on signal quality for a circular cylinder with slit.

The Modified Quality Coefficient (M_{mod}) - in detail described in [6] - is a quality parameter defined on the basis of the spectrum of the measuring signal. It takes into consideration not only the content of noise in the signal but also its frequency distribution. The Gaussian weighting function for the frequency components of the measuring signal has been applied.

$$M_{mod} = \frac{P_0}{\sum_{i=1}^{n} P_i w_i}, \tag{1}$$

where:

$$w_i = \begin{cases} exp\left[-2.83\left(\frac{f_i}{f_0}-1\right)^2\right] \\ exp\left[-2.83\left(\frac{f_0}{f_i}-1\right)^2\right] \end{cases}.$$

As seen in Fig. 10, the M_{mod} increase at short distances from the bluff body follows the rotation energy increase. Also the signal quality decrease at larger distances corresponds with the results of simulation. These results are also consistent with Bearman's investigations [7]. He has proved experimentally that the fully-developed vortex appears at a certain distance downstream the bluff body.

The results of the simulation are also closely consistent with previously obtained velocity field investigations with the application of the hot-wire anemometer (Fig. 11) [4]. A visible transverse and lengthways velocity decrease in the closest neighbourhood of the bluff body confirms the existence of the stagnation region. In this way the assumptions of the model concerning the stagnation region existence have been experimentally confirmed.

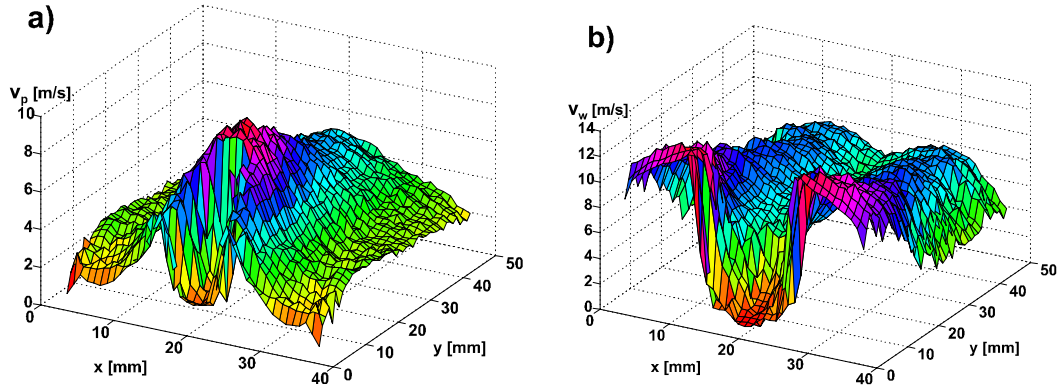

Fig. 11. Mean velocity distributions - transverse (v_p) and lengthways (v_w) - in the axial plane perpendicular to the bluff body axis.

Comparing the results of numerical simulation of convection velocity (Fig. 12) with those obtained by the flow visualization and image processing application (Fig. 13), the similarity of both graphs should be noted. It is characteristic that the convection velocity strongly increases at a certain distance downstream the bluff body and then becomes stable. It is worth noting that for both: simulation and experiment, the zone of stable convection velocity begins at the same distance from the bluff body. It confirms also the correctness of the assumption in the numerical model concerning the length of the intensive development zone.

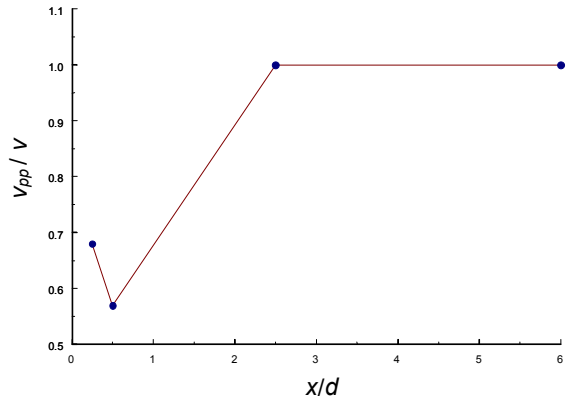

Fig. 12. Normalized convection velocity vs. normalized distance from the bluff body (results of simulation).

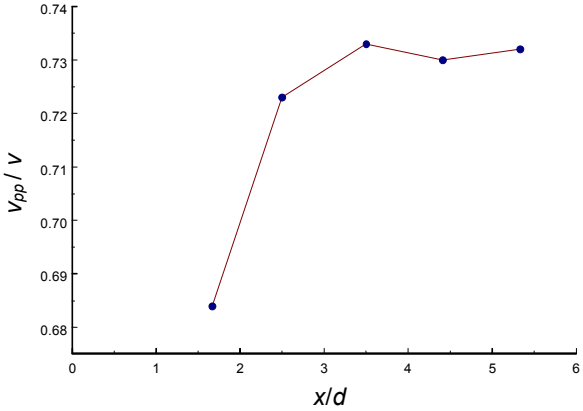

Fig. 13. Normalized convection velocity vs. normalized distance from the bluff body (experimental results obtained by flow visualization and image processing).

5. CONCLUSIONS

A simplified numerical model of the Karman vortex street based on fundamental hydromechanical equations has been developed. In spite of obvious simplifications (like e.g. sharply marked borders between particular regions and zones of vortex development), the consistence of the results of simulations and observations of the vortex Karman street properties was found remarkable. Particularly it concerns the vortex development and its energy growth in the zone close to the bluff body as well as the vortex decay in further evolution. Viscosity forces implemented into the model do not influence the vortex frequency at all but only the rotation energy losses. It is also important that the vortex development is not only a boundary layer effect, but takes place in a certain area downstream the bluff body. Hence, conclusions concerning the optimal sensor location may be formulated.

Results of numerical simulation have been compared with experimental results obtained with the application of various research methods. The methods were: meter calibration on the measuring stand, hot-wire anemometry, flow visualization with image processing. Considerable consistency has been attained. The most significant conclusions are as follows:

- the vortex develops at a certain distance downstream the bluff body,
- the maximum of the vortex rotation energy appears outside the bluff body,
- the existence of the stagnation region downstream the bluff body has been confirmed,
- the convection velocity increases downstream the bluff body and then becames stable.

Finally, on the basis of the obtained results, it can be supposed that due to a model improvement, further understanding of the complicated phenomena occurring in the vortex meter is feasible.

Due to obtained results, practical recommendations to the vortex meter design can be formulated. For instance, the most favourable secondary device location is placed at a certain distance downstream the bluff body. It is worth to note that the choice of the secondary device (from the point of view of the measuring signal magnitude) is rather critical because of considerable variation of vortex rotation energy.

NOTATION

v - flow velocity upstream the bluff body
v_{pc} - flow velocity 'driving' the vortex
v_{pp} - vortex translation velocity
ω - vortex angular velocity
x - current vortex displacement from the bluff body axis
x_s - length of intensive development zone
x_k - length of intensive development and stabilization zones
d - bluff body diameter
D - width of the pipe
r - radius of the vortex
η - dynamic viscosity
E_{rot} - rotation energy of the layer
E_{tot} - total rotation energy
k - layer number
M_{mod} - modified quality coefficient
P_0 - power contained in main spectral line
P_i - power contained in i spectral line
f_0 - frequency of main spectral line
f_i - frequency of i spectral line
v_p - transverse velocity
v_w - lengthways velocity

REFERENCES

1. Pankanin G.L. Berlinski J., Chmielewski R.: *Analytical modeling of Karman vortex street*. Metrology and Measurement Systems, vol. 12, no. 4/2005, pp.413-425.
2. Birkhoff G.: *Formation vortex street*. Journal of Applied Physics 24, no. 1 (1953).
3. Berliński J., Chmielewski R., Pankanin G.L.: *Vortex Flow Field Investigations with Application of Hot-Wire Anemometer*. Proc. of International Conference of Flow Measurement FLOMEKO 2000, Salvador, 6-10 May 2000, Brazil, CD-Rom proceedings.
4. Pankanin G.L., Berliński J., Chmielewski R.: *Karman Vortex Street Visualization*. Proc. of International Symposium on Flow Visualization, Edinburgh 26-29 August 2000, UK, paper no. 239, CD-Rom proceedings.
5. Pankanin G. L.: *The Vortex Flowmeter: Various Methods of Investigating Phenomena*. Measurement Science and Technology 16, no. 3 (2005) R1-R16 (Review article).
6. Pankanin G.L., Pytlak T.: *New Development in Vortex Meter Design*. Proc. of International Symposium on Fluid Control Measurement, Mechanics and Flow Visualisation FLUCOME'88, Sheffield, UK, pp. 479-483.
7. Bearman P.W.: *Investigation of the flow behind a two-dimensional model with a blunt trailing edge and fitted with splitter plates*. Journal of Fluid Mechanics vol. 21, part 2, 1965, pp. 241-255.

SYMULACJA ROZBUDOWY ALEI WIROWEJ KARMANA Z ZASTOSOWANIEM NOWEGO MODELU

Streszczenie

Artykuł jest poświęcony symulacji numerycznej według analitycznego modelu ścieżki wirowej Karmana szczegółowo opisanego w [1]. Przeprowadzono symulację podstawowych wielkości występujących w modelu, takich jak prędkość napędzająca wir, prędkość obrotowa wiru, czy też energia ruchu obrotowego. Przeanalizowano wpływ lepkości płynu na właściwości zjawiska. Uzyskano dobrą zgodność wyników symulacji z wynikami uzyskanymi z wykorzystaniem innych metod badawczych.